AIAA JOURNAL
Vol. 40, No. 11, November 2002

Error Control and Adaptivity for Low-Mach-Number Compressible Flows

Murat Sabanca,* Gunther Brenner,† and Franz Durst‡
Friedrichs–Alexander University, D-91058 Erlangen, Germany

An error estimation and grid adaptation strategy is presented for low-Mach-number, compressible, isentropic flows in two dimensions. There is very little literature investigating error control and grid refinement strategies combined with low-Mach-number compressible flows simultaneously, although these two concepts have been treated separately. The error control and the refinement procedure is based on the adjoint formulation in which the adjoint function is connected to local residual error, as well as linear variation of the functional with respect to a coarse grid solution. The benefit of the presented local grid refinement strategy based on some prechosen relevant engineering quantity is that it quantifies the specific locations in the domain that most affect the approximation of this quantity while maintaining the computational efficiency. Moreover, this approach is broader in the sense of not requiring a priori knowledge of the flow compared to standard gradient-based or global refinement approaches. Finally, the predictive capability of the error estimation strategy is demonstrated quantitatively by comparing to experimental and theoretical results for flows past slender bumps and a National Aerospace Laboratory NLR7301 multi-element airfoil for Mach numbers from 0.001 to 0.185.

Nomenclature

C_p	=	pressure coefficient
c	=	forces
c_d	=	drag coefficient
c_l	=	lift coefficient
E	=	total internal energy per unit volume
e	=	total energy per unit mass
H	=	total enthalpy
h	=	specific enthalpy
I	=	output functional
J_1	=	cost functional at the suction point
J_2	=	cost functional at the stagnation point
M	=	Hessian matrix
Ma	=	Mach number
P	=	pressure
Q	=	vector of conservative variables
$\boldsymbol{Q}$	=	total quality parameter
q	=	local quality parameter
T	=	triangle
t	=	time
U_i, U_j	=	cartesian components of velocity
V	=	adjoint function
v	=	edge array
x	=	abscissa
y	=	ordinate
α	=	angle of attack, rad
γ	=	specific heat ratio, c_p/c_v
ϵ	=	discretization error
η	=	error criterion
ρ	=	density
τ	=	bump thickness
Φ	=	numerical flux function
∞	=	freestream values

Subscripts

a	=	axial component
D_p	=	pressure drag force
e	=	stagnation point
F	=	inviscid fluxes
I	=	interpolation error
i	=	ith Cartesian component
j	=	jth Cartesian component
k	=	average value
l	=	lower surface
n	=	normal component
s	=	suction point
u	=	upper surface
0	=	initial state

Superscripts

h	=	approximate solution
-1	=	inverse of the matrix
$-$	=	edge averaging

Introduction

THE compressible form of the Euler equations allows two types of propagation speeds, the speed of sound and the speed of flow. In the case of low-Mach-number flows, such as chemically reacting flows in combustion chambers or landing and takeoff configurations of multi-element airfoils, the speed of sound is much higher than the flow speed. The flow is almost incompressible. This leads to numerical simulation problems when applying the fully compressible form of the Euler equations to low-Mach-number flows. However, there exist remarkable improvements in this field by using approximate Riemann solvers, although the wave structure of approximate Riemann solvers is still an open question in multiple dimensions (see Refs. 1 and 2). In such situations, the loss of accuracy is critical and is often the limiting factor, when applying computational fluid dynamics as a design or an analysis tool. The recent developments[3–6] in the design and the implementation of the finite volume methods for the Euler equations in the low-Mach-number regime allow us to apply residual driven a posteriori mesh refinement to overcome accuracy problem. Nowadays, it is possible to simulate unsteady, viscous low-Mach-number flows to investigate the compressible effects at high-temperature ratios with compressible solvers[7] or steady viscous flows with chemical reactions at a high rate of density fluctuations.[8]

Received 18 October 2001; revision received 24 March 2002; accepted for publication 3 May 2002.

*Research Scientist, Institute of Fluid Mechanics, Paul-Gordan Strasse 3, D-91052 Erlangen. Member AIAA.

†Senior Research Scientist, Institute of Fluid Mechanics, Paul-Gordan Strasse 3, D-91052 Erlangen.

‡Professor, Institute of Fluid Mechanics, Cauer Strasse 4.

The developments in computer technology as well as in the design and the implementation of algorithms allow ever larger, more complex problems to be handled. This increase in the dimension and the complexity can be compensated and predicted accurately by solving for a large number of unknowns. The concepts of error control and adaptivity, whose tools were already known from solid mechanics,[9,10] have been already utilized for wide range of flow situations in the finite element framework by Strouboulis and Oden,[11] Becker and Rannacher,[12] Giles et al.,[13] Ilinca et al.,[14] Peraire et al.,[15] and Braack and Rannacher.[8]

However, it has been bypassed for low-Mach-number compressible cases. This problem was first attacked by Braack and Rannacher[8] and Becker and Rannacher[12] by simplifying the full compressible Navier–Stokes equations at low Mach numbers for steady, viscous chemically reacting cases. A Galerkin-type finite element (FE) algorithm was utilized to solve the set of equations for both the flow variables and the variables controlling the discretization errors. The flow variables were taken as dual functions of simplified Navier–Stokes equations, and the refinement of the grid was utilized with respect to a posteriori solution of the dual formulation of the governing equations.

On the other hand, for finite volume (FV) simulations, several techniques for numerically estimating the discretization error were introduced by Pierce and Giles,[16] Giles and Pierce,[17] Van Straalen et al.,[18] Sabanca et al.,[19] and Venditti and Darmofal.[20,21] The refinement strategies for FV formulations have been concentrated on residual approximation, gradient-based flow variable approximations, accurate approximation of relevant engineering quantities, and reduction of global discretization error. Among the strategies, the accurate estimation of relevant engineering quantities on the basis of variation of the residual with respect to dual function is promising because there are usually a few integral quantities of primary concern such as lift and drag coefficient on an aircraft. The rest of the solution is often needed only for qualitative purposes, for example, to see if there is a bad flow separation. The aim of the present study is to estimate these integral quantities accurately at low-Mach-number flows by using a modified FV, approximate Riemann solver in two dimensions for transient or steady applications. The low-Mach-number simulation with an approximate Riemann solver is a stiff problem if the fastest wave travels from one end to the other end of a two-dimensional virtual shock tube and sweeps out the undisturbed region that is used to guess the solution. From this point of view, it is a reasonable approach to use anisotropic grids. (The smaller the Mach number is, the more stretched are the grids in the convection direction.) In this case, it seems unfavorable to enrich the mesh points. However, this problem is not so easy to avoid by a simple grid trick for low-Mach-number compressible cases. Nevertheless, the idea behind anisotropic grids is used to check the quality of the meshes in calculating the interpolation errors and to derive a total mesh quality parameter for the computations by constructing a Hessian matrix on each edge with respect to the interpolated flow variable (see Peraire et al.[15] and Dolejši[22]).

Error control and adaptivity for a wide range of high subsonic, isentropic transonic, and shocked flow cases for inviscid quasi-one-dimensional flows were reported by Venditti and Darmofal.[20,21] The well known approximate Riemann solver of Roe[2] was utilized to solve the governing equations. The error control and the adaptivity are assessed through accurate computation of pressure. The exact error in the computations is estimated by using the Richardson extrapolation. A very crucial yet usually overlooked disadvantage of the Richardson extrapolation is that the extrapolated solution generally is not conservative in the sense of maintaining conservation properties (see Roache[23]). To reach an all-Mach-number capability, the conserved variables were used for both governing and adjoint equations in the present study. That is why the Richardson extrapolation was unsuitable for the present investigation. Because the canonical form of the Euler equations is hyperbolic in space and is solved along infinitely many characteristic directions, the corresponding error estimation strategies are more difficult in the FV framework compared to one-dimensional cases, which have only two characteristic directions. The present study can be seen as a completing work in the field of refinement strategies by covering slightly compressible (almost incompressible), multidimensional cases with a slightly different and simpler technique than that of Venditti and Darmofal[20,21] that can readily be implemented on an existing all-Mach-number-capable solver.

The plan of the paper is as follows. In the next section, we will mention the well-known Euler equations as well as the boundary conditions and briefly explain the time discretization. In the succeeding section, the proposed iterative grid refinement strategy to improve the approximation of relevant engineering quantities in the low-Mach-number cases will be explained. The refinement strategy will be based on the accurate computation of lift and drag coefficients. Then, in the next section, from the standard interpolation error reduction concept, the total mesh quality parameter will be derived to rank the overall quality of the meshes in the computations. The low-speed, most-cited geometries in the literature are chosen as test cases to measure the quantitative accuracy of the lift and drag computations, as well as the predictive capability of the error estimation technique. The results will then be shown.

Governing Equations

The equations governing the inviscid, compressible, and isentropic flows are written as follows:

$$\frac{\partial \rho}{\partial t} + \frac{\partial (\rho U_i)}{\partial x_i} = 0 \tag{1}$$

$$\frac{\partial (\rho U_j)}{\partial t} + \frac{\partial (\rho U_i U_j)}{\partial x_i} = -\frac{\partial P}{\partial x_j} \tag{2}$$

$$\frac{\partial (\rho E)}{\partial t} + \frac{\partial (\rho E U_i)}{\partial x_i} = -P \frac{\partial U_i}{\partial x_i} \tag{3}$$

where $i, j = 1, 2$. The equations of state to compute the pressure and the equation for total enthalpy are given as

$$P = (\gamma - 1)\left[\rho E - \rho\left(U_1^2 + U_2^2\right)/2\right], \qquad H = E + P/\rho$$

Equations (1–3) are solved numerically by using a third-order spatially accurate cell vertex scheme with a modified approximate Riemann solver at low Mach numbers (see Roe[2] and Sabanca et al.[5]).

Boundary Conditions and Time Discretization

The inlet and outlet boundary conditions are based on the characteristic directions between the ghost nodes, which have the freestream values, and the boundary nodes.[24] A Neumann-type boundary condition, namely, the slip wall, is utilized on the wall boundaries. The discrete form of the governing equations in time is a variant of the approximate factorization algorithm (locally implicit but globally explicit). The solution procedure is based on the Riemann problem at the cell interfaces. The procedure posed for the approximate solution is for the infinite domain, and thus, interactions among waves are precluded. The waves from other faces within a control volume should not reach to another face. This implies that the time step Δt is limited so that wave interactions do not occur. More specifically, the fastest wave should not reach from one face to the neighboring faces in Δt. It turns out that this constraint is compatible with the classical Courant–Friedrichs–Lewy condition for conditional stability (see Venkatakrishnan and Mavripilis[25]).

Error Control and Refinement Strategy

The error control and the refinement strategy utilized in the present study is a discrete adjoint formulation.[20] After that, the solution adaptive refinements based on this discrete method are compared with a gradient-based method that utilizes a Hessian matrix and with a global refinement. Assuming $Q = [\rho, \rho U_1, \rho U_2, \rho E]$ to be the exact solution and Q^h the approximate solution of Eqs. (1–3), we obtain the residual for Q^h as

$$\mathrm{res}(Q^h) = \Phi_F\left(Q^h, n_i\right) \tag{4}$$

where Φ_F is the inviscid modified numerical flux function.[2,5] The linear approximation to the exact value of res(Q) is

$$\mathrm{res}(Q) \approx \mathrm{res}(Q^h) + \frac{\partial \mathrm{res}}{\partial Q^h}(Q - Q^h) \tag{5}$$

Because the present study deals with time-independent applications, the value of the residual (res) for the exact solution must be zero, that is, $\text{res}(Q) = 0$. Then the discretization error from Eq. (5) becomes

$$\epsilon = Q - Q^h = -\left(\frac{\partial \text{res}}{\partial Q^h}\right)^{-1} \text{res}(Q^h) \tag{6}$$

When Eq. (6) is followed, the relation between the discretization error and the relevant engineering parameters such as lift and drag can be explained as follows: The total pressure forces exerted by the fluid on the airfoil are composed of a horizontal c_a^h and a vertical c_n^h component. If these pressure forces are integrated from the leading edge (LE) to the trailing edge (TE), one obtains

$$c_n^h = -\int_{\text{LE}}^{\text{TE}} \left[C_{p,l}(Q^h) - C_{p,u}(Q^h)\right] \mathrm{d}x \tag{7}$$

$$c_a^h = -\int_{\text{LE}}^{\text{TE}} \left[C_{p,u}(Q^h)\frac{\mathrm{d}y_u}{\mathrm{d}x} - C_{p,l}\frac{\mathrm{d}y_l}{\mathrm{d}x}\right] \mathrm{d}x \tag{8}$$

where subscripts l and u stand for the lower and upper surfaces of the airfoil, respectively. When the component of forces normal to and parallel to the chord are taken,

$$c_l^h(Q^h) = c_n^h \cos(\alpha) - c_a^h \sin(\alpha) \tag{9}$$

$$c_d^h(Q^h) = c_n^h \sin(\alpha) + c_a^h \cos(\alpha) \tag{10}$$

As one notices, although the computations are carried out by using the inviscid flow model, there is a nonzero drag coefficient as a result of the contribution of the pressure forces.

If $I_h(Q^h) = [c_l^h, c_d^h]$, the output functional, is the lift or drag obtained from the discretization of the approximate solution and the $I(Q)$ the exact solution, then the error in the approximation of these engineering relevant quantities is

$$I_h(Q^h) - I(Q) = \underbrace{\left[I_h(Q^h) - I_h(Q)\right]}_{\text{computable error}} + \underbrace{\left[I_h(Q) - I(Q)\right]}_{\text{negligible error}} \tag{11}$$

The second term in Eq. (11), the error of the integral operator, is assumed to be negligible if the integral is approximated with enough points by using left or right Riemann sum or trapezoid rule. The first term is the dominant error term from the discrete solution. The linearization of the adjoint arguments around the numerical solution and substitution of Eq. (6) results in[13]

$$I_h(Q^h) - I_h(Q) \approx \left.\frac{\partial I_h}{\partial Q}\right|_{Q=Q^h} (Q - Q^h)$$

$$= \underbrace{-\left.\frac{\partial I_h}{\partial Q}\right|_{Q=Q^h} \left[\frac{\partial \text{res}(Q^h)}{\partial Q^h}\right]^{-1}}_{V} \text{res}(Q^h) = \boldsymbol{V}\text{res}(Q^h) \tag{12}$$

where the vector $\boldsymbol{V}$ is the solution of the adjoint flow equations,

$$\left[\frac{\partial \text{res}(Q^h)}{\partial Q^h}\right]\boldsymbol{V} + \frac{\partial I_h}{\partial Q^h} = 0 \tag{13}$$

Thus, the adjoint flow solution relates the errors in quantities such as lift and drag to the underlying truncation errors in the evaluation of FV residuals. The refinement strategy will, of course, depend on the nature of the criterion of accuracy that we wish to satisfy. A very common requirement from solid mechanics is to specify the achievement of a certain minimum percentage error in the energy (or L_2) norm.[9] In Eq. (12), $\boldsymbol{V}$ is the approximation to the adjoint solution in terms of adjoint arguments, here lift or drag coefficients, and weights the residual locally in the vicinity of the wall nodes. Having obtained the solution on the coarse grid, the postprocessing of the solution is fulfilled with respect to an a priori given tolerance (tol)

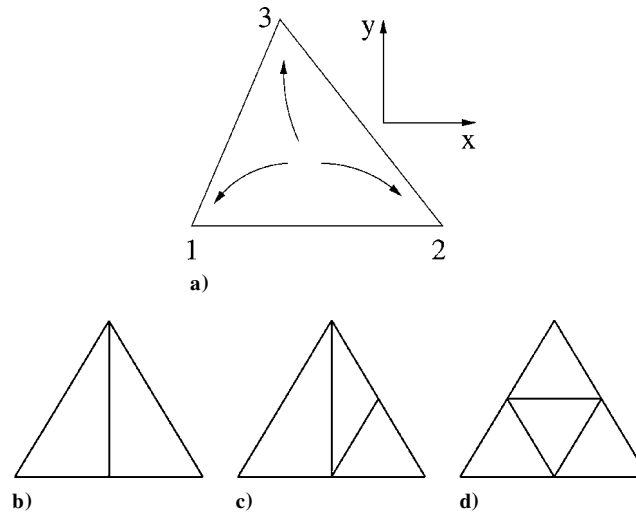

Fig. 1 Mesh a) optimality based on interpolation and b), c), and d) refinement.

value as follows: triangles whose η values satisfy the condition for a given tol value,

$$\eta = \epsilon \frac{\text{area}(T)}{\text{float(number of grid points)}} \geq \text{tol} \tag{14}$$

are marked for refinement. The marked triangles are divided by joining the midpoints of the edges as is shown in Fig. 1d, regular refinement. After this type of refinement, we get hanging nodes in some triangles. To get rid of this problem, the triangles having exactly one hanging node are bisected by joining the hanging node to the vertex opposite to it (Fig. 1b). The triangles that have two hanging nodes are divided by joining the hanging node to the midpoint of the longest edge and the latter to the opposite vertex, as is shown in Fig. 1c (Ref. 26). This process is repeated until an approximately constant value of the weighted error is obtained in the entire domain. At this stage of the solution, an overrefinement of the grid might be a problem. This problem can be avoided by using a suitable tolerance value as stopping condition. Moreover, in the present investigations, the horizontal component of the momentum equations and the lift coefficient are used as key variables in the refinement of the grids.

What Is the Overall Quality of the Triangles?

In this section, we describe the mathematical background of the anisotropic meshes and derive a quality parameter for the meshes used in the present investigations. The interpolation error ϵ_I for linear interpolation of flow variables in the FV frame is

$$\epsilon_I = \frac{1}{2}\left[\frac{\partial^2 Q^h(x, y_i, t_0)}{\partial x^2}(x - x_i)^2 + 2\frac{\partial^2 Q^h(x, y_i, t_0)}{\partial x \partial y}(x - x_i)(y - y_i) + \frac{\partial^2 Q^h(x_i, y, t_0)}{\partial y^2}(y - y_i)^2\right] + \mathcal{O}\left(|x - x_i, y - y_i|^3\right), \qquad i = 1, 2, 3 \tag{15}$$

The points satisfying Eq. (15) form an ellipse in contrast to Delaunay's circumcircular formulation. For any edge in Fig. 1a, the array $\boldsymbol{v} = (x - x_i, y - y_i)$ and the positive-definite Hessian matrix are defined as

$$M = \begin{pmatrix} \dfrac{\partial^2 Q^h}{\partial x^2} & \dfrac{\partial^2 Q^h}{\partial x \partial y} \\ \dfrac{\partial^2 Q^h}{\partial x \partial y} & \dfrac{\partial^2 Q^h}{\partial y^2} \end{pmatrix} \tag{16}$$

In the computation of M, a standard central discretization method on the triangles is utilized. The interpolation error given in Eq. (15) can be expressed as

$$\|v\|_M = (vMv^T)^{\frac{1}{2}} \tag{17}$$

If we consider the triangle in Fig. 1a for any edge E_k of the triangle, the M matrix is averaged on the edge, $\overline{M_k} = \frac{1}{2}(M_i + M_j)$. The triangle is optimal if $\|E_k\|_{\overline{M_k}} = \sqrt{3}, k = 1, 2, 3$. Then the optimality parameter for a triangle is measured by

$$q_T = \left[\sum_{k=1}^{3} \left(\|E_k\| - \sqrt{3} \right)^2 \right]^{\frac{1}{2}} \tag{18}$$

The total quality of the mesh is defined by

$$Q_T = \frac{1}{\text{float(number of triangles)}} \sum_T q_T \tag{19}$$

It is clear that $Q_T > 0$ and that the mesh is optimal if $Q_T = 0$. The Hessian matrix M defined by Eq. (16) can be evaluated for all of the conserved variables. However, this is not the case in the present study. For the gradient-based approach, this matrix is evaluated with respect to a key variable, which is the horizontal component of the momentum, that is, ρU_1.

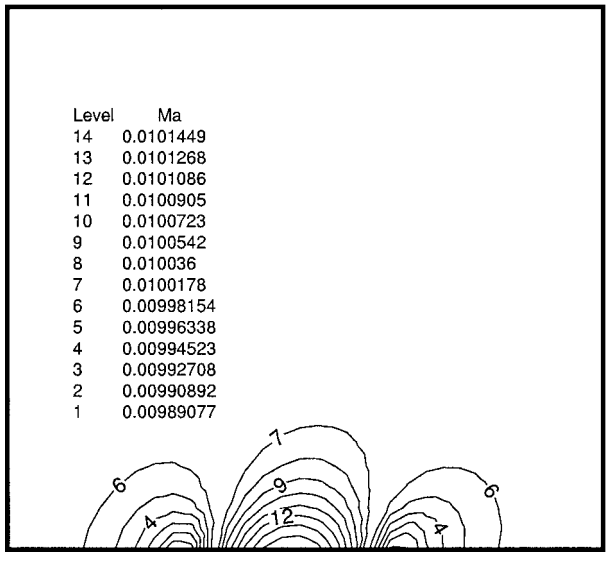

Fig. 2a Mach contours for case 22.

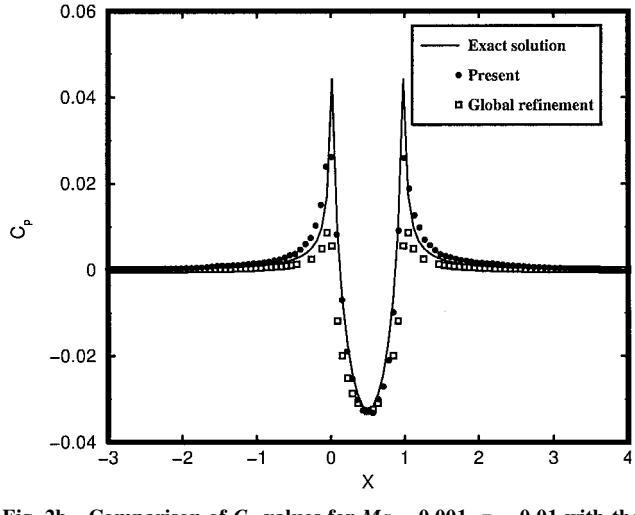

Fig. 2b Comparison of C_p values for Ma = 0.001, τ = 0.01 with the theoretical result.[28]

Results and Discussion

The theoretical work mentioned in the previous sections was applied to the test cases that are shown in Table 1 and to a multielement National Aerospace Laboratory airfoil NLR7301 at high angles of attack. These test cases have been cited most in the literature, especially 10% bump[27] for high subsonic and transonic applications. Moreover, in any standard text book of gasdynamics, one can see the theoretical solutions for flow past slender bumps.[28] On the other hand, the low-speed, high-lift NLR7301 airfoil with flap, which is one of the most cited geometries, is chosen to measure the quantitative accuracy of the lift and drag coefficients, as well as the predictive capability of the error estimation technique.

Flow Around a Bump in a Channel

The very low-Mach-number subsonic flow over the bump shows the expected theoretical behavior: increasing velocity in the forward

Table 1 Test cases: bump thicknesses τ vs Mach numbers

	Case number		
τ	$Ma_\infty = 0.1$	$Ma_\infty = 0.01$	$Ma_\infty = 0.001$
0.1	11	21	31
0.01	12	22	32
0.001	13	23	33

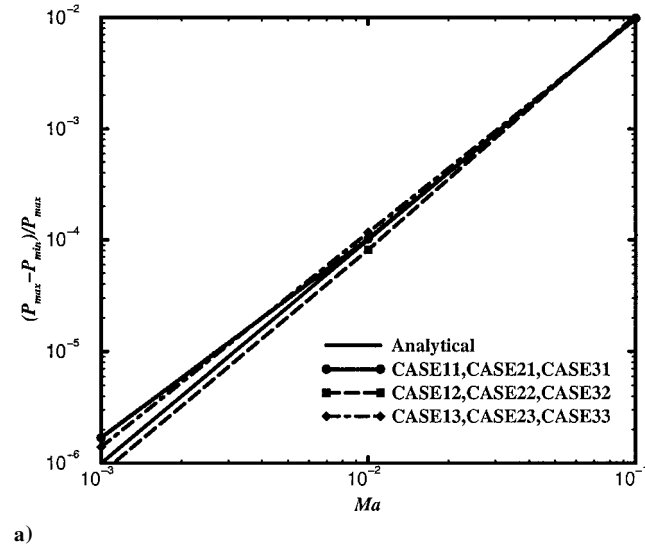

a)

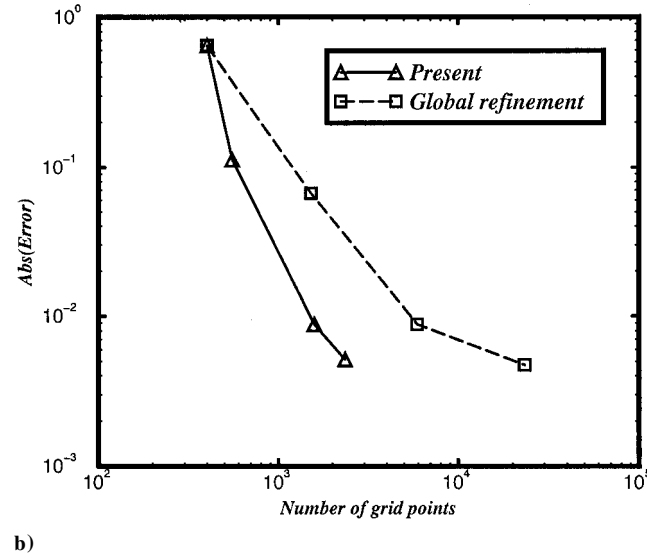

b)

Fig. 3 Case 22: a) comparison of pressure oscillations with the theoretical work and b) comparison of the error (momentum) for local and global refinements.

portion of the bump and the decreasing velocity in the rear half portion. In the middle of the bump, the pressure reaches its local minimum value, as shown in Figs. 2a and 2b (Ref. 28). Moreover, the present local refinement approach is compared to the global refinement strategy in Fig. 2b. In the vicinity of stagnation points, the outlined method gives slightly better results than the global refinement strategy with fewer grid points. The mesh quality parameter Q_T for this case is found to be 1.984 as the best value after four cycles of refinement. In accordance with the theory summarized by Van Dyke,[29] the asymptotic expansion of the flow variables with respect to Mach number shows that the pressure oscillations at Mach numbers as $Ma \to 0$ should be directly proportional to $\mathcal{O}(Ma^2)$, as is shown in Fig. 3a. Figure 3b shows error reduction for both the present local refinement approach and the global refinement strategy for case 22. The initial grid has 400 nodes. After a four-level uniform grid refinement, the same level of error reduction is obtained with approximately 10 times fewer grid points. The error map shown in Fig. 4a for case 22 corresponds to error distribution on the initial coarse grid with respect to key variable ρU_1. After that, this initial coarse grid is refined four cycles with tol = 0.01, and as is shown by the corresponding error map with respect to ρU_1 in Fig. 4b, the present approach is capable to reduce the error.

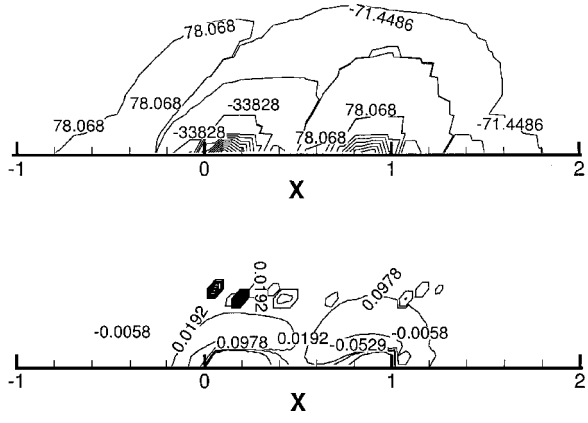

Fig. 4 Error maps for case 22 a) before refinement and b) after four cycles of refinement.

NLR7301 Airfoil

The computed surface pressure distributions for incidence angles of 6 and 13.1 deg for the flow around the low-speed, high-lift NLR7301 airfoil/TE flap configuration of Van den Berg[30] are shown in Figs. 5a and 5b. This is a landing/takeoff configuration with the flap angle 20 deg and with the largest flap gap 2.6%. The experiment was carried out in a low-speed wind tunnel with $Ma = 0.185$ and Reynolds number 2.51×10^6. The difference between the experimental and the computational results on the upper surface of the elements shown in Figs. 5a and 5b results from the thick boundary-layer development in the flow. Because in the present study only inviscid flows are considered, this effect cannot be reproduced. However, the agreement between the inviscid calculation and the experiment is remarkable. The grid-enrichment strategy increases the number of

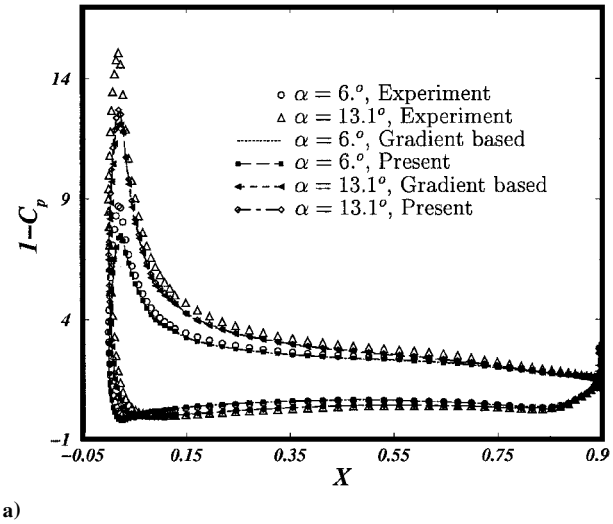

Fig. 5 Comparison of the $1 - C_p$ distribution a) on the main element and b) on the flap element for angle of incidences, $\alpha = 6$ and 13.1 deg.

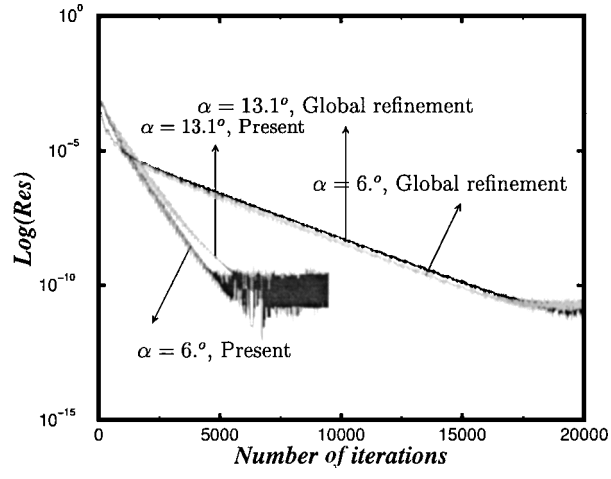

Fig. 6a Comparison of convergence histories for the present and global refinements.

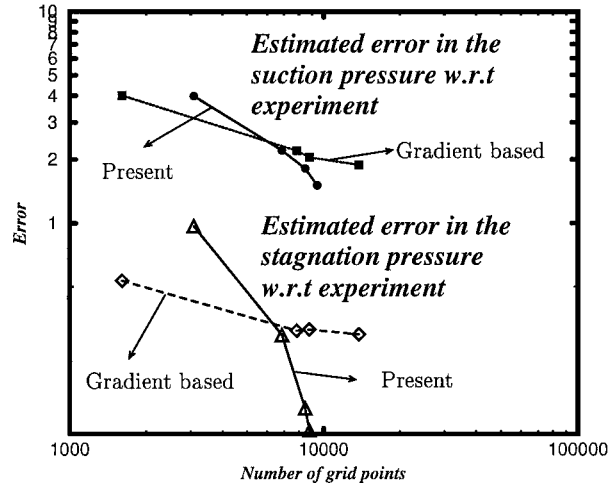

Fig. 6b Results of the computation of the error functional for suction and stagnation points, α = 13.1 deg.

unknowns to be solved, and as the number of unknowns increases, the time needed to reach a steady-state solution increases. A comparison between the present local grid refinement strategy and the global mesh enrichment is shown in Fig. 6a. If we take a cost functional J_1 as the difference between the correct (experimental) suction pressure P_s and the computed suction pressure p at the suction point of main element, then

$$J_1(\phi_F) = \begin{cases} (P_s - p) & \text{at the suction point} \\ 0 & \text{otherwise} \end{cases} \tag{20}$$

If we do the same thing for the stagnation pressure on the flap element where P_e is correct (or experimental) stagnation pressure for which the cost functional J_2 is defined as

$$J_2(\phi_F) = \begin{cases} (P_e - p) & \text{at the stagnation point} \\ 0 & \text{otherwise} \end{cases} \tag{21}$$

then the present approach's superiority of the predictive capability in estimating the dominant pressure terms on the gradient-based approach is as shown in Fig. 6b. The reason is that the pressure gradients are strong in the gap between the main and the upper forward portion of the flap element where the fluid is compressed; however, the maximum stagnation point at this angle of incidence, $\alpha = 13.1$ deg, is on the lower forward portion of the TE flap. The overall mesh quality before the refinement decreases from $Q_T = 8.194$ to 4.284 and after third refinement to $Q_T = 2.994$ for this case. Figure 7a shows the expected behavior of the flow around a high-lift airfoil, low pressure on the upper half portion of the airfoil and high pressure on the lower surface. The NLR7301 at high angle of incidence experiences a stagnation point on the front portion, as well as on the flap element. The pressure reaches its minimum at the suction point. Figure 7b shows the predictive capability of the present approach quantitatively.[30] The difference is due to thick boundary-layer development on the upper surface of the configuration and the incapability of the inviscid flow model to solve the boundary layer.

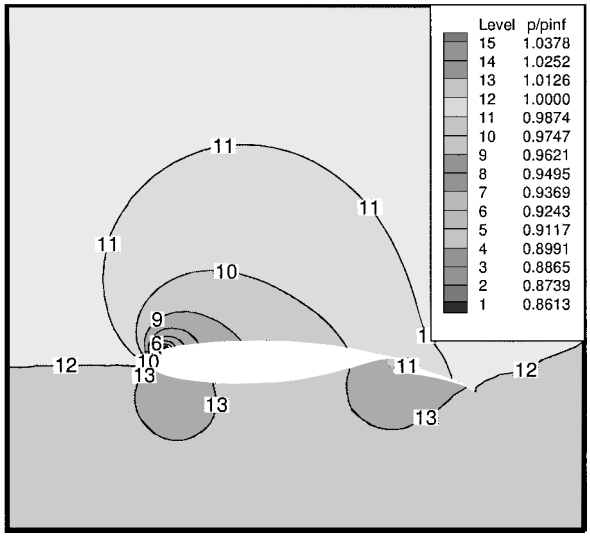

Fig. 7a Pressure contours for NLR7301, $\alpha = 6$ deg.

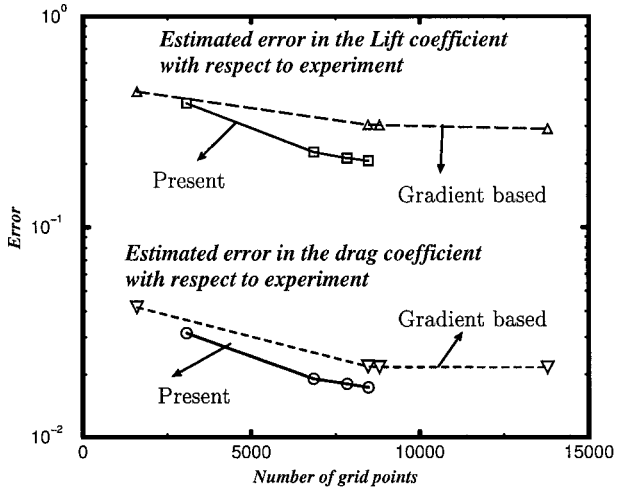

Fig. 7b Comparison of c_l^h and c_d^h with experimental measurements of Van den Berg,[30] with $C_l = 3.15$, $C_d = 0.048$, and $\alpha = 13.1$ deg.

Conclusions

The solutions of refinement procedures based on error estimation techniques for the accurate solutions of slightly compressible flows over the slender bumps as well as flows past a multi-element airfoil agree well with the previous experimental and theoretical results. The predictive capability of the adjoint formulation, in which the adjoint function is connected to local residual error as well as linear variation of the functional with respect to coarse grid solution, is more accurate than gradient-based techniques and more efficient than global refinement strategies. The difference between the experimental and the computational results on the upper surface of the multi-element airfoil is not a result of inexact error estimation. However, it results from the thick boundary-layer development in the flow, which cannot be handled by the inviscid flow model. The benefit of the presented local grid-refinement strategy based on some prechosen relevant engineering quantity is that it quantifies the specific locations in the domain that affect most the approximation of this quantity while maintaining the computational efficiency. Moreover, this approach is broader in the sense of not requiring a priori knowledge of the flow compared to standard gradient-based or global refinement approaches.

References

[1]Munz, C. D., and Klein, R., "The Multi Pressure Variable Approach for the Numerical Approximation of Weakly Compressible Fluid Flow," Proceedings of the International Conf. on Numerical Methods for Fluid Flows, Prague, June 1995.

[2]Roe, P. L., "Approximate Riemann Solvers, Parameter Vectors, and Difference Schemes," *Journal of Computational Physics*, Vol. 43, Oct. 1981, pp. 357–372.

[3]Choi, D., and Merkle, C. L., "Application of Time-Iterative Schemes to Incompressible Flow," *AIAA Journal*, Vol. 23, No. 10, 1985, pp. 1518–1524.

[4]Darmofal, D. L., and Schmid, P. J., "The Importance of Eigenvectors for Local Preconditioners of the Euler Equations," *Journal of Computational Physics*, Vol. 127, No. 2, 1996, pp. 346–362.

[5]Sabanca, M., Brenner, G., and Alemdaroğlu, N., "Improvements to Compressible Euler Methods for Low Mach Number Flows," *International Journal for Numerical Methods in Fluids*, Vol. 34, No. 2, 2000, pp. 167–185.

[6]Turkel, E., "Preconditioned Methods for solving the Incompressible and Low Speed Compressible Equations," *Journal of Computational Physics*, Vol. 72, 1987, pp. 277–298.

[7]Sabanca, M., Brenner, G., and Durst, F., "Slight Compressible Effects for Flows around Circular Cylinders at High Temperature Ratios," Third International Symposium on Finite Volumes, June 2002.

[8]Braack, M., and Rannacher, R., "Adaptive Finite Element Methods for Low Mach Number Flows with Chemical Reactions," *30th Computational Fluid Dynamics*, Vol. 3, von Kármán Inst. Lecture Series, von Kármán Inst., Rhode-Saint-Genése, Belgium, 1999, pp. 1–93.

[9]Zienkiewicz, O. C., and Zhu, J. Z., "A Simple Error Estimator and Adaptive Procedure for Practical Engineering Problems," *International Journal for Numerical Methods in Engineering*, Vol. 24, 1987, pp. 337–357.

[10]Babuška, I., and Miller, A., "The Post Processing Approach in the Finite Element Method—Part 1: Calculation of the Displacements, Stresses and Other Higher Order Derivatives of the Displacements," *International Journal for Numerical Methods in Engineering*, Vol. 20, 1984, p. 1085.

[11]Strouboulis, T., and Oden, J. T., "A Posteriori Error Estimation of Finite Element Approximations in Fluid Mechanics," *Computational Methods in Applied Mechanics and Engineering*, Vol. 78, 1990, pp. 201–242.

[12]Becker, R., and Rannacher, R., "Weighted A Posteriori Error Control in FE Methods," *ENUMATH-97*, World Scientific, Singapore, 1998.

[13]Giles, B. M., Larson, M. G., Levenstam, J. M., and Süli, E., "Adaptive Error Control for FE Approximations of the Lift and Drag in Viscous Flow," Oxford Univ., COMLAB NA-Rept. 97/06, Oxford, June 1997.

[14]Ilinca, F., Pelletier, D., and Ignat, L., "Adaptive Finite Element Solution of Compressible Turbulent Flows," *AIAA Journal*, Vol. 36, No. 12, 1998, pp. 2187–2194.

[15]Peraire, J., Vahdati, M., Morgan, K., and Zienkiewicz, O. C., "Adaptive Remeshing for Compressible Flow Computations," *Journal of Computational Physics*, Vol. 72, No. 2, 1987, pp. 449–466.

[16]Pierce, N. A., and Giles, M. B., "Adjoint Recovery of Superconvergent Functionals from PDE Equations," *SIAM Review*, Vol. 42, 2000, p. 247.

[17]Giles, B. M., and Pierce, N. A., "Adjoint Equations in CFD: Duality, Boundary Conditions and Solution Behaviour," AIAA Paper 97-1850, 1997.

[18]Van Straalen, B. P., Simpson, R. B., and Stubley, G. D., "A Posteriori Error Estimation for Finite Volume Simulations of Fluid Flow Transport," *Proceedings of the Third Annual Conference*, Vol. 1, Computational Fluid Dynamics Society, Alberta, Canada, 1995.

[19]Sabanca, M., Brenner, G., Durst, F., and Tremel, U., "Adaptive Solutions of Compressible Navier–Stokes Equations in the Low Mach Number Limit Through Weighted A Posteriori Error Estimate," *ENUMATH-99*, World Scientific, Singapore, 1999, pp. 171–179.

[20]Venditti, D. A., and Darmofal, D. L., "Adjoint Error Estimation and Grid Adaptation for Functional Outputs: Application to Quasi One-Dimensional Flow," *Journal of Computational Physics*, Vol. 164, 2000, pp. 204–227.

[21]Venditti, D. A., and Darmofal, D. L., "Grid Adaptation Methodology for Functional Outputs of Compressible Flow Simulations," AIAA Paper 2001-2659, 2001.

[22]Dolejši, V., "Anisotropic Mesh Adaptation for Finite-Volume and Finite-Element Methods on Triangular Meshes," *Computing and Visualisation in Science*, Vol. 1, 1998, pp. 165–178.

[23]Roache, P. J., "Perspective: A Method for Uniform Reporting of Grid Refinement Studies," *Journal of Fluids Engineering*, Vol. 116, 1994, pp. 405–413.

[24]Steger, J. L., and Warming, R. F., "Flux Vector Splitting of the Inviscid Gasdynamic Equations with Application to Finite-Difference Methods," *Journal of Computational Physics*, Vol. 40, 1981, pp. 263–293.

[25]Venkatakrishnan, V., and Mavripilis, D. J., "Solution Techniques for Unstructured Grid Flow Computations," *Frontiers of Computational Fluid Dynamics*, Wiley, New York, 1994, pp. 135–151.

[26]Bank, R. E., Sherman, A. H., and Weiser, H.,"Refinement Algorithms and Data Structures for Regular Local Mesh Refinement," edited by R. Stepleman, *Scientific Computing*, North-Holland, Amsterdam, 1983, pp. 3–17.

[27]Ni, R. H., "Multiple-Grid Scheme for Solving the Euler Equations," *AIAA Journal*, Vol. 20, No. 11, 1982, pp. 1565–1571.

[28]Zierep, J., *Theoretische Gasdynamik*, 3rd ed., Braun, Karlsruhe, Germany, 1976, pp. 134–177.

[29]Van Dyke, M., "Perturbation Methods in Fluid Mechanics," *Applied Mathematics and Mechanics*, 3rd ed., Academic Press, New York, 1964.

[30]Van den Berg, B., "Boundary Layer Measurements on a Two Dimensional Wing with Flap," National Aerospace Lab., NLR TR 79009U, The Netherlands, 1979.

J. Kallinderis
Associate Editor